MAGNETIC STRATIGRAPHY OF THE MIDDLE MIOCENE BOPESTA FORMATION, SOUTHERN SIERRA NEVADA, CALIFORNIA

Sean Coles and Donald R. Prothero
Department of Geology
Occidental College
Los Angeles, CA 90041

James P. Quinn
Vertebrate Paleontology Section
Natural History Museum of Los Angeles County
900 Exposition Blvd.
Los Angeles, CA 90007

Carl C. Swisher, III
Berkeley Geochronology Center
2455 Ridge Road
Berkeley, CA 94709

ABSTRACT

The middle Miocene Bopesta Formation consists of over 640 m of fluvial, lacustrine, and volcaniclastic sediments and interbedded volcanics, exposed in the southern Sierra Nevada south of Cache Peak. It contains both late Hemingfordian and early Barstovian faunas, especially horses. Precise chronostratigraphy of the Bopesta Formation is important, because it lies between Miocene faunas from the Basin and Range province (Barstow, Ricardo) and Transverse Ranges (Tejon Hills, Cuyama Badlands) which have previously been sampled for magnetic stratigraphy.

Magnetic sampling was conducted on the neostratotype section that spans the thickest part of the sequence in Pine Tree Canyon, and at the late Hemingfordian Phillips Ranch locality in Sand Canyon. After removal of overprinting, the primary component of magnetization passed a reversal test, and showed no significant tectonic rotation (within the error estimates). Based on comparisons with the recently revised (Woodburne and Swisher, 1995; Woodburne, 1996) magnetic stratigraphy and biostratigraphy of the Barstow Formation, the simplest interpretation suggests that the Bopesta Formation spans Chrons C5ADn to C5Cn (14.5-16.5 Ma). A new K-Ar date on the Kinnick Tuff in the Phillips Ranch locality yielded ages of 16.5 ± 0.2 Ma on biotite and 16.5 ± 0.8 Ma on hornblende, consistent with the late Hemingfordian age of the fauna. The boundary between the late Hemingfordian *Parapliohippus carrizoensis* zone and the early Barstovian "*Merychippus*" *stylodontus* zone falls in early Chron C5Br (about 15.9 Ma), as it does in the Barstow Formation (as shown by the transition from the Rak Division to Green Hills Faunas).

INTRODUCTION

The middle Miocene was an important time in Cenozoic history. Glaciation returned to Antarctica after a brief warming episode in the early Miocene, and the South Pole has been frozen ever since. As a consequence, global climate went through a major episode of cooling and drying, causing an expansion of dry-adapted, more open vegetation at the expense of densely forested habitats (Retallack, 1990). Many changes occurred in the land mammals, including the diversification of horses and camels with longer limbs and higher-crowned teeth (Tedford and others, 1987; MacFadden, 1992).

Several places in southern California preserve an excellent record of the middle Miocene (Fig. 1), including the lower-middle Miocene Barstow Formation in the Mojave Desert (type area of the

In Gary H. Girty, Richard E. Hanson, and John D. Cooper, Eds., 1997,
Geology of The Western Cordillera: Perspectives from Undergraduate Research.
Pacific Section S.E.P.M, Vol. 82, p. 21-34.

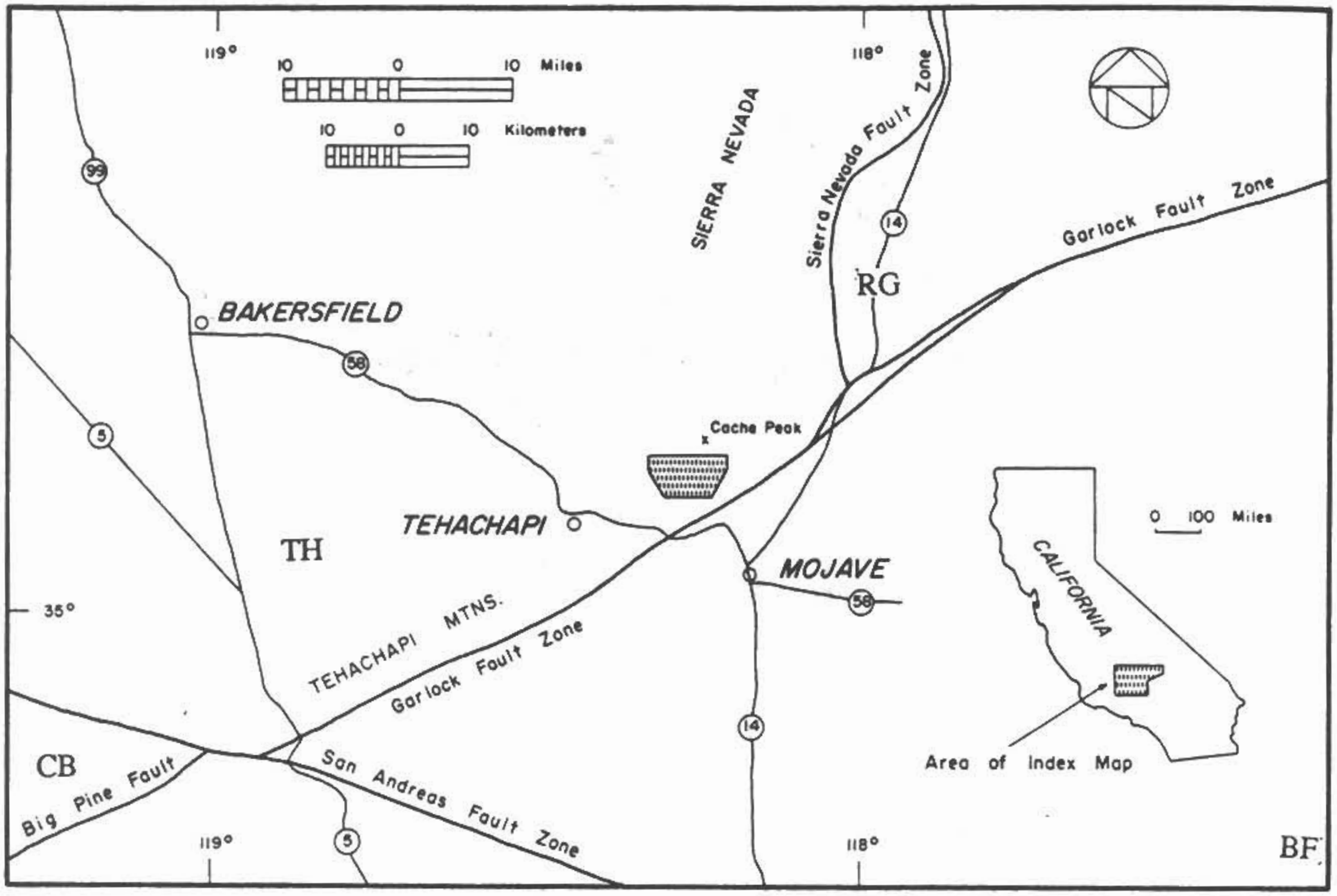

Figure 1. Index map showing the location of the Bopesta Formation (shaded area), as well as the Ricardo Group (RG) in Red Rock Canyon, the Barstow Formation (BF), the Tejon Hills (TH), and the Cuyama Badlands (CB). After Quinn (1987, fig. 1).

middle Miocene Barstovian land mammal "age") (Lindsay, 1972; Woodburne and Tedford, 1982; Tedford and others, 1987; Woodburne and others, 1990; MacFadden and others, 1990), the middle-upper Miocene Ricardo Group in Redrock Canyon in the El Paso Mountains (Burbank and Whistler, 1987; Loomis and Burbank, 1988; Whistler and Burbank, 1992), the middle-upper Miocene Tejon Hills sequence in the southeastern San Joaquin Valley (Savage, 1955; Tedford and others, 1987; Wilson and Prothero, this volume), and the lower-upper Miocene Caliente Formation in the Cuyama Badlands of the northern Transverse Ranges (James, 1963; Tedford and others, 1987; Kelly and Lander, 1988).

Another important middle Miocene sequence of mammals is known from the Bopesta Formation, located in the southernmost Sierra Nevada just north of the Tehachapi Mountains and the Garlock fault (Fig. 1). Tertiary rocks were first mentioned in the area by Lawson (1906), and the geology and fossil mammals were described in detail by Buwalda (1916, 1934, 1935, 1954; Buwalda and Lewis, 1955). The Phillips Ranch flora was described by Axelrod (1939). Reconnaissance geologic maps of this area were published by Dibblee (1959, 1967) and Dibblee and Louke (1970). All of this research was summarized, updated, and considerably expanded upon by Quinn (1987), and this work formed the basis for our research.

Most of the Miocene sequences mentioned

above have now been sampled for magnetic stratigraphy, allowing much more precise correlations to the global time scale. The magnetic stratigraphy of the Barstow Formation was studied by MacFadden and others (1990) and revised by Woodburne and Swisher (1995) and Woodburne (1996), the Ricardo Group by Burbank and Whistler (1987), Loomis and Burbank (1988) and Whistler and Burbank (1992), and the Tejon Hills sequence by Wilson and Prothero (this volume). The paleomagnetism of the Caliente Formation in the Cuyama Badlands is presently under study by K. A. McCardel, D.R. Prothero, and E. L.Wilson (in prep.). In this context, magnetostratigraphy of the Bopesta Formation will further enhance our understanding of the chronostratigraphy and faunal change that occurred during the Miocene in California.

In addition to correlation by magnetic stratigraphy, Bopesta Formation paleomagnetism could potentially provide data bearing on another interesting geologic problem. Paleomagnetic studies have shown that most of the Miocene and younger rocks of the Transverse Ranges south of the San Andreas fault are tectonically rotated clockwise by approximately 90° (Luyendyk and others, 1980; Luyendyk, 1991). However, regions north of the San Andreas fault have different histories. The Ricardo Group, which is also north of the Garlock Fault, has as much as 30° of Miocene counterclockwise rotation (Burbank and Whistler, 1987; Loomis and Burbank, 1988). The Barstow Formation in the middle of the Mojave Desert shows negligible tectonic rotation (MacFadden and others, 1990). Cretaceous rocks in the Tehachapi Mountains south of the White Wolf-Kern Canyon fault system and north of the Garlock fault show approximately 45° of clockwise rotation (Kanter and McWilliams, 1982; McWilliams and Li, 1985), but the overlying Miocene and younger rocks in this area show no significant tectonic rotation (McWilliams and Li, 1985; Wilson and Prothero, this volume). The Bopesta Formation is also between the White Wolf and Garlock faults, so it should not show any tectonic rotation, and our data will test this hypothesis.

THE BOPESTA FORMATION

The Bopesta Formation is part of a thick Tertiary sequence in the Cache Peak area (Quinn, 1987). In stratigraphic order, this sequence consists of the early Tertiary (?Paleocene Goler Formation equivalent) Witnet Formation (about 1200 m of sandstone and conglomerate), the lower Miocene Kinnick Formation (about 1300 m of sandstone, mudstone, basalt flows, and volcaniclastic rock), the middle Miocene Bopesta Formation (over 640 m of fluvial, lacustrine, and volcaniclastic sediment, and interbedded volcanics), and the post-middle Miocene (possibly ?Pliocene) Cache Peak Formation (about 200 m of agglomerates, breccias, and flows). Quinn (1987) subdivided the Bopesta Formation into four informal members. The lower member (Tbl) consists of up to 87 m of sandstone, siltstone, mudstone, and volcaniclastic rock deposited in a fluvial and volcanic setting. It overlies the highest basalt of the Kinnick Formation (Tk10), and interfingers with and is capped by a distinctive unit of agglomerates and breccias (Tbi). The middle member (Tbm) reaches a maximum of 305 m in thickness, and is composed mostly of volcanic sandstone, mudstone, and chert, largely deposited in fluvial and lacustrine environments. It is separated from the upper member (Tbu) by a distinctive lapilli tuff. The upper member reaches a maximum of 241 m in thickness, and consists mostly of floodplain mudstone and sandstone, with very little volcanic input (for further details, see Quinn, 1987).

Quinn (1987) located many new fossil sites, as well as most of the previously discovered localities, on his maps and sections. For our purposes, two sections covered the key fossiliferous intervals in the Bopesta Formation. We sampled the 40 m of strata that encompass the late Hemingfordian Phillips Ranch fauna and flora, also known as University of California, Berkeley, Museum of Paleontology (UCMP) locality V-2577, and Los Angeles County Museum-California Institute of Technology locality LACM(CIT) 503. It is located in Sand Canyon (SE NE and N 1/2 Sec. 33, T31S R34E, Tehachapi NE 7.5' Quadrangle, Kern County, California). We also sampled the thickest, most complete section of the Bopesta Formation along Quinn's (1987) neostratotype section in Pine Tree Canyon, located along a transect from NW Sec. 4, T22S R35E, to SE Sec. 32, T31S R35E, Cache Peak 7.5' Quadrangle, Kern County, California (route of section shown in Quinn, 1987, Plate II, Section II). Together, these sections can be tied to many of the key fossil localities, and allow the biostratigraphy of the formation to be tied directly to the magnetic stratigraphy.

Table 1.

KA no.	Material Dated	Weight (grams)	%K mean	$^{40}Ar^*$ (mol/g)	$\%^{40}Ar^*$	Age Ma ± SD
478-2	biotite	0.49396	6.2601	1.801-10	78.8	16.52 ± 0.22
5365	hornblende	1.31267	0.4745	1.368-11	29.3	16.55 ± 0.84

METHODS

Stratigraphic sections were measured using a Jacob's staff, compensating for the dip and for recognized faults. Four magnetic sites were collected in the 40-m-thick Phillips Ranch section, and 36 sites were collected at 15 to 20 m intervals to cover the 700 m of the neostratotype section. Three block samples were collected per site, using simple hand tools, and later subsampled into 2.5-cm cubes using a band saw with a tungsten-carbide blade. The samples were measured with the 2G cryogenic magnetometer at the California Institute of Technology paleomagnetics laboratory. The NRM (natural remanent magnetization) of each sample was measured, and then the sample was demagnetized with alternating fields (AF) of 25, 50, and 100 Gauss to demagnetize any multi-domain grains, and to determine the coercivity behavior of each sample. After AF demagnetization, each sample was then thermally demagnetized at 300°, 400°, 500°, and 600°C in a magnetically shielded furnace. This dehydrates any iron hydroxides such as goethite, removing their remanence, and also allows determination of how much magnetization remained above the Curie temperature of magnetite (580°C).

In addition to the detailed AF and thermal demagnetization of each sample, about 0.1 g of several samples were powdered and placed in epindorph tubes for rock magnetic analyses. Each powdered sample was subjected to increasing IRM (isothermal remanent magnetization), and the peak IRM and ARM (anhysteretic remanent magnetization) was subjected to AF demagnetization in a modified Lowrie-Fuller test (see Pluhar and others, 1991, for further details).

In addition to the studies outlined above, several polished thin sections of representative lithologies were examined under reflected light using an oil-immersion lens to determine the magnetic mineralogy.

RESULTS

Geochronology

An important calibration point for the late Hemingfordian faunas characterized by *Parapliohippus carrizoensis* has been the age of the Kinnick Tuff, which underlies the Phillips Ranch fauna. Evernden and others (1964) reported a K-Ar biotite age of 17.6 Ma. The Phillips Ranch fauna is similar to the Red Division fauna of the Barstow Formation, which lies just below the Rak Tuff, which yields a $^{40}Ar/^{39}Ar$ date of 15.88 ± 0.06 Ma (MacFadden and others, 1990; Woodburne and Swisher, 1995). Because the Phillips Ranch fauna is above the 17.6 Ma date on the Kinnick Tuff, and the Rak Tuff is above the Red Division fauna, this information does not preclude that either of the dates is incorrect, although it would suggest that this fauna spanned at least 1.5 million years. To see if we could refine this age difference, the Kinnick Tuff was redated.

Examination of the biotite separate dated by Evernden and others (1964) revealed adhering devitrified glass on dark, fresh-looking biotite, iron oxide grains, and approximately 10% hornblende. The biotite separate was improved by removing the adhering glass with a ball mill and sonic cleaner, and separating the biotite from the hornblende with MEI. Both the biotite and hornblende were dated by K-Ar methods. Analysis of the biotite yielded 6.3% potassium and 79% radiogenic argon for an age of 16.5 ± 0.2 Ma (Table 1). Evernden and others (1964) reported a potassium content of 5.18% and 66% radiogenic argon, yielding their age estimate of 17.6 Ma.

Support for the accuracy of this younger age was obtained by dating the hornblende that was removed from the biotite separate. The resultant K-Ar date of 16.5 ± 0.8 Ma (Table 1) is concordant with the 16.5 ± 0.2 Ma age on the biotite. These dates indicate that the date by Evernden and others (1964) on the Kinnick Tuff was approximately 1.1

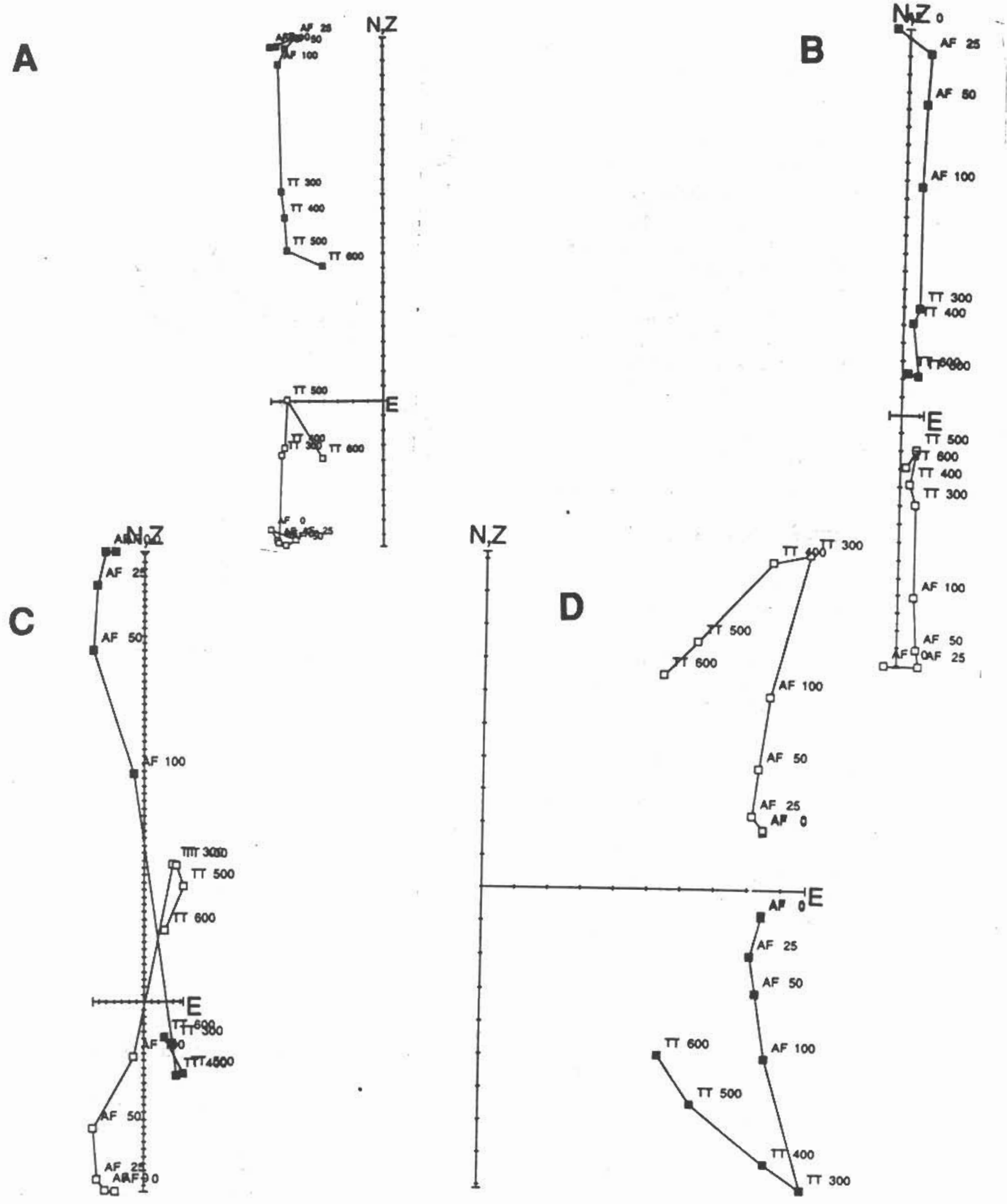

Figure 2. Orthogonal demagnetization ("Zijderveld") plots of representative samples. Solid squares indicate declination; open squares indicate inclination. "AF" indicates alternating field demagnetization step in Gauss; "TT" indicates thermal demagnetization step in degrees Centigrade. Each division equals 1 x 10^{-6} emu (1 x 10^{-9} Am^2) in Fig. 2A, 1 x 10^{-5} emu (1 x 10^{-8} Am^2) in the remaining figures.

million years too old. Our explanation for the older age is: 1) samples were heterogeneous, containing biotite, glass, and hornblende, which resulted in lower potassium values and lower amounts of radiogenic argon; 2) improved methods of potassium analyses for iron-bearing minerals, such as biotite, indicate that some potassium analyses included in the study of Evernden and others (1964) were on the order of 1% too low (pers. commun. with Jochim Hampel, who did the potassium analyses). These low potassium values yielded artificially old ages. If the potassium and radiogenic argon values varied proportionally, then our ages should be concordant with those of Evernden and others (1964). We measured a greater amount of radiogenic argon, which would have the effect of an older age. However, we also measured a proportionally higher percentage of potassium, which resulted in a net younger age.

Magnetic Analyses

The magnetic behavior of each sample was plotted on an orthogonal demagnetization, or "Zijderveld" plot (Fig. 2). The horizontal component (declination, D) of the sample is shown with the solid squares, and the vertical component of magnetization is indicated by the open squares. Sample 3B (Fig. 2A) shows a typical normally magnetized sample which did not respond to AF treatment, indicating the presence of a high-coercivity mineral such as goethite or hematite; this is also suggested by the high remanence left at 500° and 600°C. Sample 29A (Fig. 2B) is normally magnetized, but reponded readily to AF treatment and had little remanence left at 600°C, suggesting that most of its magnetization was carried in magnetite. Sample 26B (Fig. 2C) is reversely magnetized, with an overprint disappearing at 300°C; its low coercivity also suggests significant magnetite. Sample 27A (Fig. 2D) was reversed at NRM, with a normal overprint disappearing at about 300°C, and a stable reversed component (held largely in a high-coercivity mineral such as hematite) appeared between 300° and 600°C.

Rock magnetic analyses of several samples (Fig. 3), on the other hand, showed no sign of hematite, whether they were obtained from sandstones of different colors and degree of iron-oxide staining, or from volcaniclastics. All showed IRM saturation (ascending curve of open squares on right) at about 300 mT (millitesla), indicating that magnetite is the major magnetic mineral in

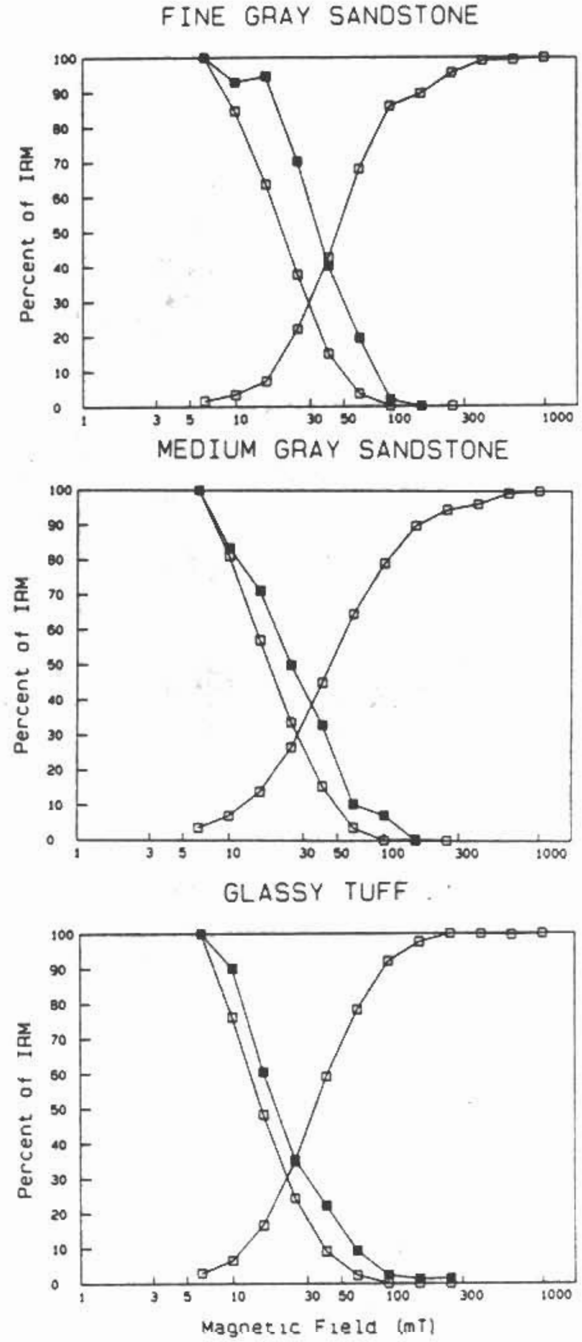

Figure 3. Rock magnetic analyses of selected samples. IRM (isothermal remanent magnetization) indicated by open squares; ARM (anhysteretic remanent magnetization) indicated by solid squares. IRM acquisition (ascending curve on right) shows saturation around 300 mT (millitesla) or 3000 Gauss, indicating that magnetite is the major carrier of remanence. The modified Lowrie-Fuller test (descending curves on left) shows that the ARM is more resistant to AF demagnetization than the IRM, suggesting that the remanence is carried by single-domain or pseudo-single-domain grains.

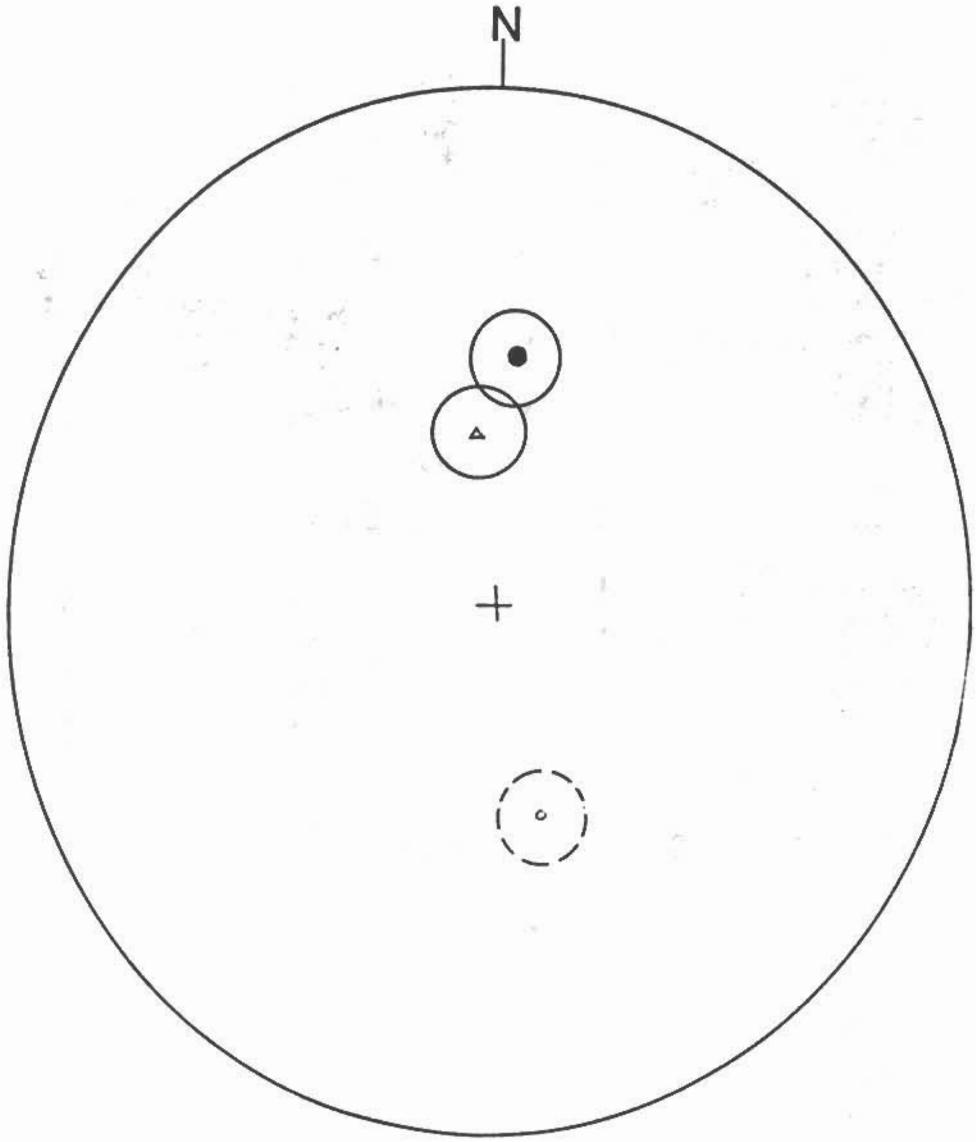

Figure 4. Stereonet showing mean direction and α_{95} circle of normal sites (solid circle and dot, lower hemisphere projection) and reversed sites (open and dashed circles, upper hemisphere projection). The mean for the reversed sites (triangle) is inverted through the center of the stereonet and overlaps the circle of confidence for the normal sites. This positive reversal test indicates that the cleanedmagnetic vectors are primary directions.

these samples. Even though some of the reddest, most iron-hydroxide-rich samples were selected, none showed the lack of IRM saturation characteristic of hematite.

In the Lowrie-Fuller test of each sample, the ARM (solid squares) is more resistant to AF demagnetization than was the IRM (open squares descending to the right), suggesting that the remanence is carried in single-domain or pseudo-single-domain grains (see Pluhar and others, 1991). This was corroborated by the polished thin sections, which revealed abundant tiny detrital magnetite grains, as well as larger, rounded, platy detrital hematite grains, which were presumably multi-domain, and thus did not retain a remanance that showed up in most of our analyses.

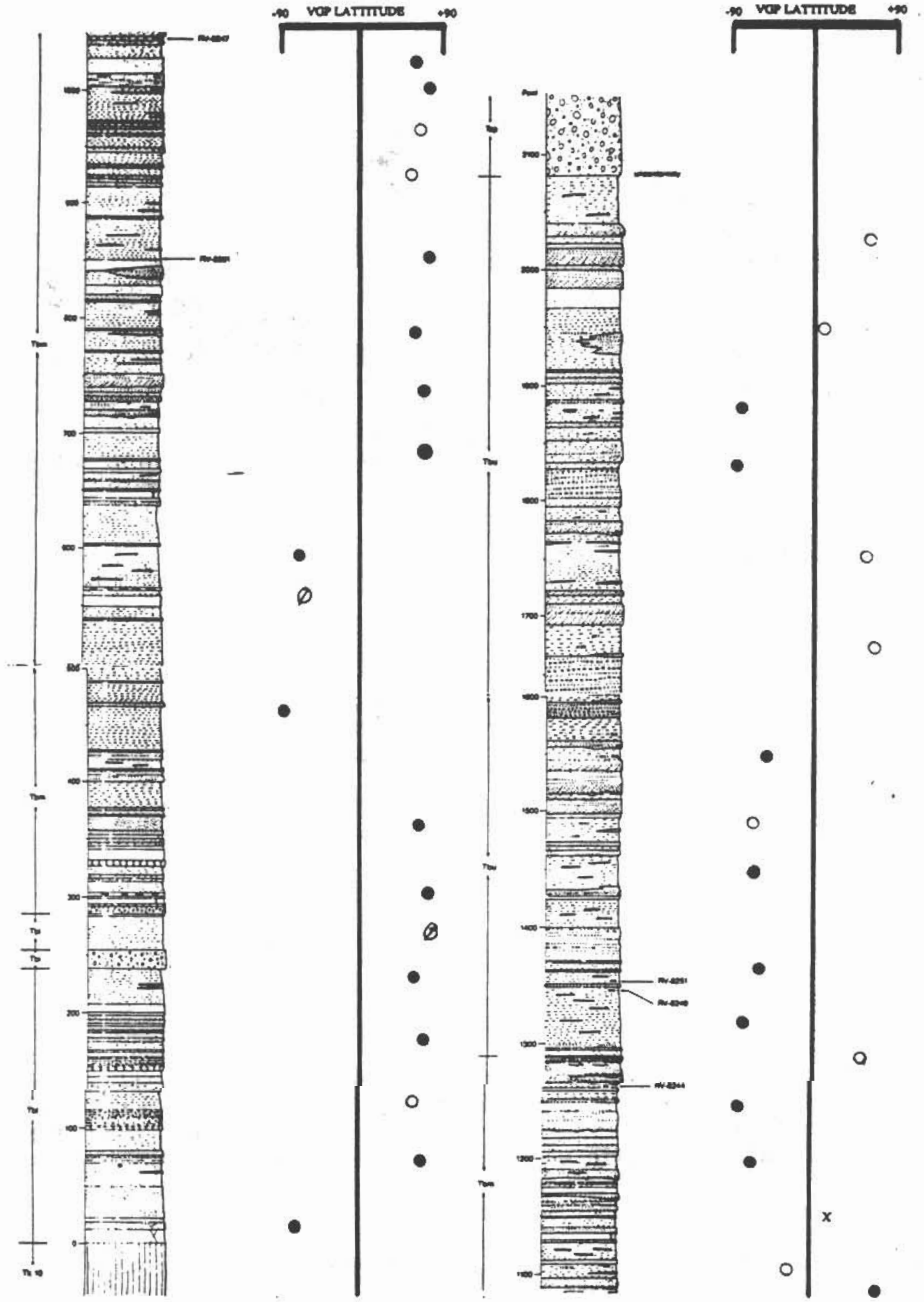

Figure 5. Magnetic stratigraphy of the neostratotype section of the Bopesta Formation (after Quinn, 1987, Plate II). Virtual geomagnetic pole (VGP) latitude is positive for normal polarity, negative for reversed polarity. Solid circles indicate Class I sites of Opdyke and others (1977). Circles with diagonal slash are Class II sites. Open circles are Class III sites. "x" indicates indeterminate site.

Based on these results, the vector component obtained between 300-500°C was used for further analyses. The three sample vectors for each site were averaged using the methods of Fisher (1953; see Butler, 1992), and classified using the scheme of Opdyke and others (1977). Class I sites (24 total) are significantly distinguished from a random scatter at the 95% confidence level. Class II sites (2 total) had only two samples remaining, so site statistics could not be calculated. Class III sites (11 total) were not significantly clustered at the 95% confidence level, since one sample from each site was divergent, but two out of three samples showed a clear polarity preference.

Although the strata dipped about 20° to the northwest in the neostratotype section, there was not enough dip variation to conduct a fold test for stability. However, the reversal test (Fig. 4) showed that the directions represent a primary or characteristic remanence, since the mean direction for the normal sites (D = 359.0°, I = 37.4°, k = 20.6, α_{95} = 9.4) was antipodal (within the error estimate) to the mean for the reversed sites (D = 171.8°, I = -49.9°, k = 22.7, α_{95}= 9.8). This error estimate is large enough to include the modern pole position for this latitude, suggesting no tectonic rotation or translation in this area. This is consistent with previous studies of the Miocene rocks of the southern Sierra Nevada and Tehachapi Mountains (McWilliams and Li, 1985; Wilson and Prothero, this volume).

Magnetic Stratigraphy

The magnetic stratigraphy of the neostratotype section is shown in Figure 5. The lowest site (just above the highest Kinnick basalt) is reversed in polarity, but the rest of the lowest 400 feet of the section (all of the Tbl, Tbi, and lower Tbm) are of normal polarity. A reversed polarity zone in the Tbm occurs between 400 and 600 feet on the neostratotype section, followed by a normal polarity zone between 600 and 1100 feet, covering the rest of the middle member. The highest part of the middle member (from 1100 feet) and the lower upper member (to 1600 feet) have a reversed polarity, and the upper part of the upper member yielded normal polarity between 1600 and 1800 feet, reversed polarity between 1800 and 1900 feet, and normal polarity to the top of the section. This polarity pattern is summarized with respect to the lithostratigraphy and fossil localities in Figure 6.

In the thinner Phillips Ranch section to the east of the neostratotype, the lowest site (including LACM(CIT)503) has a reversed polarity, but the three higher sites have a normal polarity (Fig. 7).

Figure 7 presents our correlation of the Bopesta Formation with the global time scale. This correlation relies upon the biostratigraphic correspondence between the partially coeval Bopesta Formation and the well dated Barstow Formation (see Woodburne and others, 1990; MacFadden and others, 1990; revised by Woodburne and Swisher, 1995, and Woodburne, 1996). Three stratigraphically successive biozones are recognized in the Bopesta Formation, characterized mainly by their fossil horses. These are the *Parapliohippus carrizoensis*, *"Merychippus" stylodontus*, and *"Merychippus" intermontanus* range zones (Quinn, 1987; see Kelly, 1995, for the renaming of *"Merychippus" carrizoensis*). The Hemingfordian/Barstovian land mammal "age" boundary has been tentatively placed between the *Parapliohippus carrizoensis* and *"Merychippus" stylodontus* range zones.

Woodburne and others (1990) identified five biozones in the Barstow Formation. In ascending stratigraphic order, they are the Red Division Fauna, the transitional Rak Division Fauna, the Green Hills Fauna, the Second Division Fauna, and the Barstow Fauna. Woodburne and others (1990) considered the Red Division and the Rak Division faunas to be of late Hemingfordian "age," and the Green Hills, Second Division, and Barstow faunas to be of Barstovian "age" (but see Evander, 1986, and Lindsay, 1995, for different interpretations). Based on faunal similarities, the *Parapliohippus carrizoensis* range zone is correlative with the Red Division Fauna, the *"Merychippus" stylodontus* range zone with the Green Hills Fauna, and the *"Merychippus" intermontanus* range zone with the Second Division Fauna of the Barstow Formation (Quinn, 1987).

MacFadden and others (1990) correlated the strata containing the late Hemingfordian Red Division Fauna with Chron C5C (Fig. 7). The Rak Division fauna occurs in strata of alternating normal and reversed polarities that MacFadden and others (1990) correlated with Chrons C5C and the lower part of Chron C5Br. Both of these correlations were retained by Woodburne and Swisher (1995) and Woodburne (1996).

However, Woodburne and Swisher (1995) and Woodburne (1996) have considerably revised

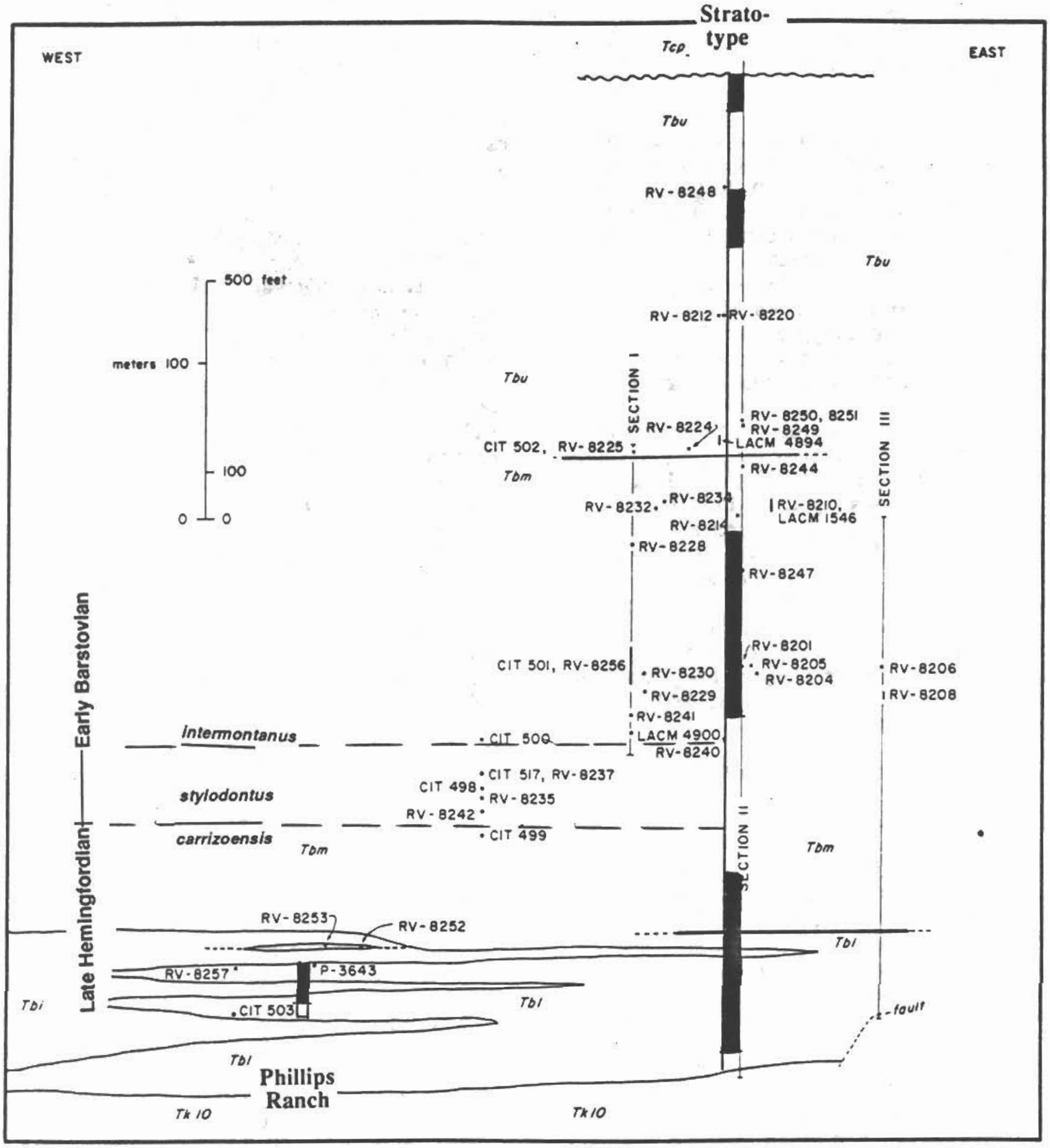

Figure 6. Biostratigraphy and lithostratigraphy of key fossil localities in the Bopesta Formation, showing the magnetic stratigraphy of the Phillips Ranch and neostratotype sections, and the position of the *Parapliohippus carrizoensis*, "*Merychippus*" *stylodontus*, and "*Merychippus*" *intermontanus* local range zones of Quinn (1987). Abbreviations of fossil localities: CIT, California Institute of Technology (now deposited at the LACM); LACM, Natural History Museum of Los Angeles County; RV, University of California, Riverside. (Modified from Quinn, 1987, fig. 31).

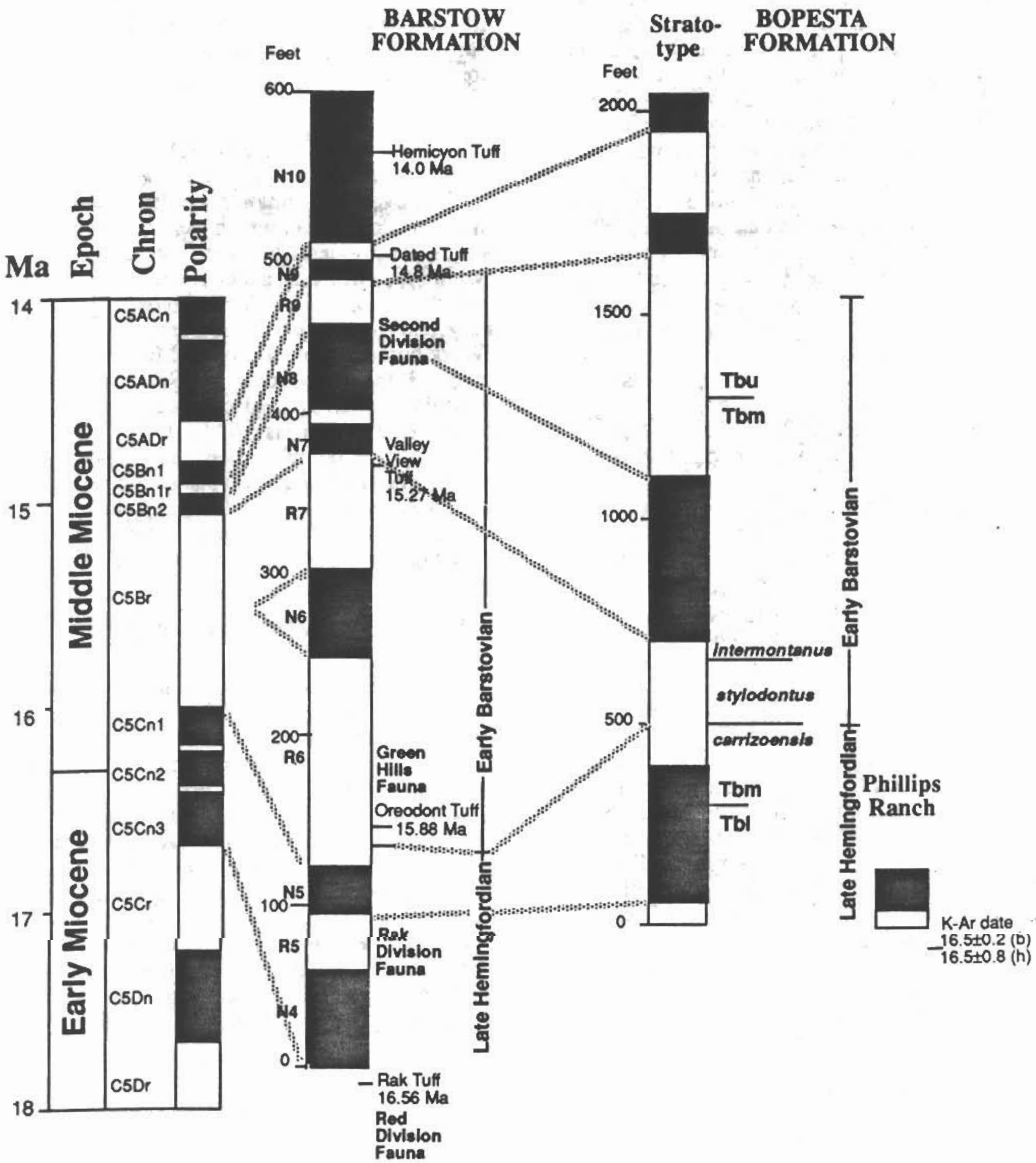

Figure 7. Correlation of the magnetic stratigraphy of the Bopesta Formation to the Barstow Formation (after MacFadden and others, 1990, revised after Woodburne and Swisher, 1995, and Woodburne, 1996), and to the magnetic polarity time scale (after Berggren and others, 1995).

the interpretation of the higher part of the Barstow section, based on new $^{40}Ar/^{39}Ar$ dates. Originally, MacFadden and others (1990) correlated the Barstovian Green Hills Fauna with Chrons C5Br and C5AD, the Second Division Fauna with Chron C5ACn, and the Barstow Fauna with Chrons C5AC to C5AB. Woodburne and Swisher (1995) and Woodburne (1996) found this correlation scheme inconsistent with the new dates (and some of the older ones), and decided that polarity zone N6 (Fig. 7) was an artifact of expanded section (or possibly due to unremoved normal overprinting?) that correlated with no chron represented on the magnetic polarity time scale. They correlated magnetozones N7 and N8 (including the Second Division Fauna and the newly dated Valley View Tuff, which yields a date of 15.27 Ma) with Chron C5Bn2 (MacFadden and others, 1990, correlated these magnetozones with Chrons C5ADn). Woodburne and Swisher (1995) and Woodburne (1996) correlated Barstow magnetozone N9 with Chron C5Bn1, which MacFadden and others (1990) correlated with part of Chron C5ADn. Woodburne and Swisher (1995) and Woodburne (1996) correlate Barstow magnetozone N10 with Chrons C5ADn and C5ACn, and suggested that C5ACr in the Barstow section may have been removed by an unconformity. MacFadden and others (1990) originally correlated N10 with C5ACn only.

In the Bopesta Formation, the *Parapliohippus carrizoensis* range zone spans a section of alternating normal and reversed polarities that we correlate with Chrons C5Cn and the lower part of C5Br. The *"Merychippus" stylodontus* range zone occurs in a section of reversed polarity that we correlate with Chron C5Br. The Hemingfordian/ Barstovian boundary (*fide* Woodburne and others, 1990) is placed in Chron C5Br in both the Bopesta and Barstow formations.

Most of the *"Merychippus" intermontanus* range zone occurs in a normal magnetozone which best correlates with Barstow normal magnetozones N7 and N8, which contains the correlative Second Division fauna. If the interpretation of Woodburne and Swisher (1995) and Woodburne (1996) is correct, then the strata producing the *"Merychippus" intermontanus* range zone in the Bopesta Formation would be expected to correlate with Chron C5Bn2.

The alternating polarity zones in the upper part of the Bopesta Formation are largely unconstrained by biostratigraphic data, but assuming no undocumented unconformities, the simplest interpretation is that they correlate with Chrons C5ADn and C5Bn1. Radiometric dating of the abundant volcanic materials in the Bopesta Formation may provide additional tests of these correlations.

CONCLUSIONS

The Bopesta Formation yielded a stable magnetic component which passed a reversal test, and showed no tectonic rotation or translation (within the error estimates). Based on correlations with the isotopically calibrated biostratigraphy and magnetic stratigraphy of the Barstow Formation (Woodburne and others, 1990; MacFadden and others, 1990; Woodburne and Swisher, 1995; Woodburne, 1996), the Bopesta Formation correlates with Chrons C5ADn to C5Cn1 (14.5-16.5 Ma). The boundary between the late Hemingfordian *Parapliohippus carrizoensis* zone and the early Barstovian *"Merychippus" stylodontus* zone falls in early Chron C5Br (about 15.9 Ma), as it does in Barstow.

ACKNOWLEDGMENTS

This research was based on an undergraduate comprehensives project by Coles, supervised by Prothero and Quinn. We thank Liz Miura, Josh Salzman, and Joey Sutton for help with sampling in this very difficult terrain. We thank Joseph Kirschvink for access to the Caltech magnetics lab, and Scott Bogue for his help with the reflected-light petrography. We thank Zond Industries for their cooperation and for access to the land. We thank Scott Bogue, Gary Girty, Richard Hanson, Tom Kelly, Monte Marshall, Dick Tedford, and Mike Woodburne for their helpful reviews of different drafts of this manuscript. This research was partially supported by NSF grant EAR94-05942 to Prothero.

REFERENCES CITED

Axelrod, D. I., 1939, A Miocene flora from the western border of the Mohave Desert: Carnegie Institution of Washington Publications, v. 516, 129 p.

Berggren, W.A., Kent, D. V., Swisher, C. C., III, and Aubry, M.-P., 1995, A revised Cenozoic geochronology and chronostratigraphy: SEPM Special Publication, v. 54, p. 129-212.

Burbank, D. W., and Whistler, D. P., 1987, Temporally constrained tectonic rotations derived from magnetostratigraphic data: implications for the initiation of the Garlock fault, California: Geology, v. 15, p. 1172-1175.

Butler, R. F., 1992, Paleomagnetism: Magnetic Domains to Geologic Terranes: Boston, Blackwell Scientific Publishers, 319 p.

Buwalda, J. P., 1916, New mammalian faunas from Miocene sediments near Tehachapi Pass in the southern Sierra Nevada: University of California Publications in Geological Sciences, v. 10, n. 6, p. 75-85.

Buwalda, J. P., 1934, Tertic tectonic activity in the Tehachapi region: Pan-American Geologist, Abstracts, v. 61, p. 309-310.

Buwalda, J. P., 1935, Tertiary tectonic activity in the Tehachapi region: Proceedings of the Geological Society of America, 1934, abstract, p. 312.

Buwalda, J. P., 1954, Geology of the Tehachapi Mountains, California: California Division of Mines and Geology Bulletin, v. 170, p. 131-142.

Buwalda, J. P., and Lewis, G. E., 1955, A new species of *Merychippus*: U. S. Geological Survey Professional Paper 264-G, p. 143-152.

Dibblee, T. W., Jr., 1959, Preliminary geologic map of the Mojave quadrangle: U. S. Geological Survey Mineral Investigation Field Studies Map MF-219.

Dibblee, T. W., Jr., 1967, Areal geology of the western Mojave Desert: U. S. Geological Survey Professional Paper 522, 153 p.

Dibblee, T. W., Jr., and Louke, G. P., 1970, Geologic map of the Tehachapi Quadrangle, Kern County, California: U. S. Geological Survey Miscellaneous Geological Investigations Map I-607.

Evander, R. L., 1986, Formal redefinition of the Hemingfordian-Barstovian land mammal age boundary: Journal of Vertebrate Paleontology, v. 6, p. 374-381.

Evernden, J. F., Savage, D. E., Curtis, G. H., and James, G. T., 1964, Potassium-argon dates and the Cenozoic mammalian chronology of North America: American Journal of Science, v. 262, p. 145-198.

Fisher, R.A., 1953, Dispersion on a sphere: Proceedings of the Royal Society, v. A217, p. 295-305.

James, G. T., 1963, Paleontology and nonmarine stratigraphy of the Cuyama Valley Badlands, California. Part I. Geology, faunal interpretations and systematic descriptions of Chiroptera, Insectivora, and Rodentia: University of California Publications in Geological Sciences, v. 45, p. 1-154.

Kanter, L. R., and McWilliams, M. O., 1982, Rotation of the southernmost Sierra Nevada, California: Journal of Geophysical Research, v. 87, n. B5, p. 3810-3830.

Kelly, T. S., 1995, New Miocene horses from the Caliente Formation, Cuyama Valley Badlands, California: Natural History Museum of Los Angeles County Contributions in Science, v. 455, p. 1-33.

Kelly, T. S., and Lander, E. B., 1988, Biostratigraphy and correlation of Hemingfordian and Barstovian land mammal assemblages, Caliente Formation, Cuyama Valley area, California: Pacific Section SEPM, v. 59, p. 1-19.

Lawson, A. C., 1906, The geomorphology of the Tehachapi Valley system: University of California Publications in Geological Sciences, v. 4, p. 397-409.

Lindsay, E. H., 1972, Small mammal fossils from the Barstow Formation, California. University of California Publications in Geological Sciences, v. 93, p. 1-104.

Lindsay, E. H., 1995, *Copemys* and the Barstovian/Hemingfordian boundary: Journal of Vertebrate Paleontology, v. 15, p. 357-368.

Loomis, D. P., and Burbank, D. W., 1988, The stratigraphic evolution of the El Paso Basin, southern California: Implications for the Miocene development of the Garlock fault and uplift of the Sierra Nevada: Geological Society of America Bulletin, v. 100, p. 12-28.

Luyendyk, B. P., 1991, A model for Neogene crustal rotations, transtension and transpression in southern California: Geological Society of America Bulletin, v. 103, p. 1528-1536.

Luyendyk, B. P., Kamerling, M. J., and Terres, R., 1980, Geometric model for Neogene crustal rotations in southern California: Geological Society of America Bulletin, v. 91, p. 211-217.

MacFadden, B. J., 1992, Fossil Horses: Cambridge, Cambridge University Press.

MacFadden, B. J., Swisher, C. C., III, Opdyke, N. D., and Woodburne, M. O., 1990, Paleomagnetism, geochronology, and possible tectonic rotation of the middle Miocene Barstow Formation, Mojave Desert, southern California: Geological Society of America Bulletin, v. 102, p. 478-493.

McWilliams, M., and Li, Y., 1985, Oroclinal bending of the southern Sierra Nevada batholith: Science, v. 230, p. 172-175.

Opdyke, N. D., Lindsay, E. H., Johnson, N. M., and Downs, T., 1977, The paleomagnetism and magnetic polarity stratigraphy of the mammal-bearing section of Anza-Borrego State Park, California: Quaternary Research, v. 7, p. 316-329.

Pluhar, C., Kirschvink, J. L., and Adams, R. W., 1991, Magnetostratigraphy and clockwise rotation of the Plio-Pleistocene Mojave River Formation, central Mojave Desert, California: San Bernardino County Museum Association Quarterly, v. 38, n. 2, p. 31-42.

Quinn, J. P., 1987, Stratigraphy of the middle Miocene Bopesta Formation, southern Sierra Nevada, California: Natural History Museum of Los Angeles County Contributions in Science, v. 393, p. 1-31.

Retallack, G., 1990, Soils of the Past: Boston, Unwin Hyman.

Savage, D. E., 1955, Nonmarine lower Pliocene sediments in California: a geochronologic-stratigraphic classification: University of California Publications in Geological Sciences, v. 31, p. 1-26.

Tedford, R. H., Galusha, T., Skinner, M. F., Taylor, B. E., Fields, R. W., Macdonald, J. R., Rensberger, J. M., Webb, S. D., and Whistler, D. P., 1987, Faunal succession and biochronology of the Arikareean through Hemphillian (late Oligocene through earliest Pliocene epochs) in North America, *in* Woodburne, M. O., ed., Cenozoic Mammals of North America, Geochronology and Biostratigraphy: Berkeley University of California Press, p. 153-210.

Whistler, D. P., and Burbank, D. W., 1992, Miocene biostratigraphy and biochronology of the Dove Spring Formation, Mojave Desert, California, and characterization of the Clarendonian mammal age (late Miocene) in California: Geological Society of America Bulletin, v. 104, p. 644-658.

Wilson, E. L., and Prothero, D. R., 1997, Magnetic stratigraphy and tectonic rotations of the middle-upper Miocene "Santa Margarita" and Chanac Formations, north-central Transverse Ranges, California: Pacific Section SEPM (this volume).

Woodburne, M. O., 1996, Precision and resolution in mammalian chronostratigraphy: principles, practices, examples: Journal of Vertebrate Paleontology, v. 16, p. 531-555.

Woodburne, M. O., and Swisher, C. C., III, 1995, Land mammal high resolution geochronology, intercontinental overland dispersals, sea level, climate, and vicariance: SEPM Special Publication, v. 54, p. 329-358.

Woodburne, M.O., and Tedford, R. H., 1982, Litho- and biostratigraphy of the Barstow Formation, Mojave Desert, California, *in* Cooper, J. D., ed., Geologic Excursions in the California Desert: Guidebook for the 78th Annual Meeting of the Cordilleran Section of the Geological Society of America, p. 65-76.

Woodburne, M. O., Tedford, R. H., and Swisher, C. C., III, 1990, Lithostratigraphy, biostratigraphy, and geochronology of the Barstow Formation, Mojave Desert, southern California: Geological Society of America Bulletin, v 102, p. 459-477.